Voltage Level Control by Grid-tied Hybrid Photovoltaic and Battery Controllers in Weak Distribution Networks with Electric Vehicles

Piyadanai Pachanapan[1,*], Tanakorn Kaewchum[1], and Sakda Somkun[2]

ARTICLE INFO

Article history:
Received: 11 February 2022
Revised: 3 March 2022
Accepted: 27 March 2022

Keywords:
Battery storage system
Electric vehicle
Over-voltage control
Photovoltaic
Under-voltage control

ABSTRACT

This paper proposes the use of grid-tied hybrid inverter with voltage controller to control the voltage level in low voltage (LV) distribution networks. The growth of photovoltaic (PV) and electric vehicle (EV) may introduce over-and under-voltage issues in LV networks, respectively. To address these voltage concerns, a two-state voltage control approach is introduced, which involves adjusting active power (*P*) and reactive power (*Q*) from a grid-tied hybrid PV-battery system. The over-voltage control is implemented by allowing the grid-tied hybrid PV-battery system to absorb *Q* and reduce *P*. On the other hand, the *P* and *Q* of the grid-tied hybrid PV-battery system must be increased to provide under-voltage control. Furthermore, the P output is adjusted by enabling the battery to charge/discharge the electricity while the power factory limitation is considered. The proposed *P(V)* and *Q(V)* droop controls are examined in both over-and under-voltage scenarios by increasing PV generation and EV charging. The voltage control performances for short and long-term voltage variations are investigated in DIgSILENT PowerFactory environment using RMS-transient and quasi-dynamic simulations. The results demonstrates that the proposed grid-tied hybrid PV-battery system with voltage controller successfully secures the voltage level within the statutory limits. This provides benefits for boosting PV and EV hosting capacity in LV networks.

1. INTRODUCTION

Since 2015, the number of residential photovoltaic (PV) systems and electric vehicles (EVs) has expanded substantially in the Greater Mekong Subregion (GMS) [1], [2]. Although the growth of PV and EVs promotes the clean environment by reducing the fossil fuel usage and carbon emissions, the high penetration of PV and EV may cause voltage problems in the low voltage (LV) networks either over-voltage or under-voltage issues, particular in rural areas with weak distribution networks.

When solar irradiance is available, the PV system generates electricity to be used in combination with the utility's electricity. As a result, PV systems can reduce electricity bills while increasing voltage at the point of common coupling (PCC). However, during periods when PV generation exceeds residential demand, high PV system penetration may cause an unacceptable voltage rise in LV networks [3]. It was found that many distribution system operators (DSOs) restrict the maximum PV installation per customer to avoid over-voltage issues. Therefore, this is one of the limitations of LV networks in terms of increasing PV hosting capacity.

With the growing popularity of EVs in recent years, a large-scale grid-connected charging of residential EVs presents challenges for LV network's voltage and thermal management [4]. According to research on residential EV charging behavior in UK and US households, charging demand is low during the day, gradually increases in the evening, and stays high at night on both weekends and weekdays [5], [6]. The study in the UK also found that the transformers and line feeders in LV networks tend to have thermal problems when EV penetrations are over 40%. Moreover, some LV networks experience under-voltage, particularly in the evening, when EV penetration is very high (> 90 %) [7]. As a result, these voltage and thermal constraints are two bottlenecks in the residential EV expansion.

Many DNOs use grid reinforcement and on-load tap changing (OLTC) fitted transformers to keep the voltage level within statutory limits. Despite the fact that grid reinforcement is effective at reducing line losses in radial LV feeders, this solution is extremely costly [8]. The primary purpose of OLTC-fitted transformers is to handle slow voltage changes caused by load variations. However, as PV and EV penetration grows, voltage variability

[1]*Department of Electrical and Computer Engineering, Faculty of Engineering, Naresuan University, Thailand*.
[2]*School of Renewable Energy and Smart Grid Technology, Naresuan University, Thailand.*
**Corresponding author:* P. Pachanapan; Phone: +66-55-96-4322; Fax: 66-55-96-4005; E-mail: piyadanip@nu.ac.th.

becomes much more severe, necessitating continuous tap changes, which raises transformer tension [9].

The voltage control can be applied locally by PV and EV customers. The over-voltage issues in LV networks can be reduced by employing the active power (P) reduction and reactive power (Q) absorption into customer owned grid-tied PV inverters. The P curtailments can be employed by many strategies [10], such as tripping PV system when over-voltage condition is met; limiting maximum power; applying fixed production based on available PV generation and adding droop control where P is a function of voltage level [$P(V)$]. Moreover, the falling price of home-scale battery energy storage (BES) is taking a new the way for future P curtailment, in which customers could locally store excess energy during high PV generation [11]. The disadvantage of P curtailment is reducing feed-in active power, which adversely affects the PV owner revenue.

The voltage level can be mitigated by drawing the Q from the main grid into the PV inverters [12]-[14]. There are two solutions for controlling the Q of PV inverters: using Q as a function of output P [$Q(P)$], and using Q as a function of voltage level [$Q(V)$]. In addition, the amount of Q supported from PV inverters is normally limited by the power factor restriction based on the Connection Agreement. This limitation further declines the PV inverters' voltage control ability. The main disadvantages of using Q compensation are that 1) it necessitates higher current flow on LV feeders, resulting in additional line losses and distribution network congestion [15], and 2) it may place additional strain on PV inverters, reducing their lifetime [16].

The centralized control solution known as "the ESPRIT technology" is employed in [4],[7] to manage the EV charging points to prevent the consequences coming from the booming of EVs. The selected EV charging points are disconnected when a technical issue, voltage or thermal problem, occurs in the LV network. Those selected EV charging points, are then reconnected once the problem has been resolved. However, customers may experience more and longer disconnections as EV adoption grows, which increases the length of charging time.

The charging load allocation strategy based on the Time-of-Use (TOU) price system can be employed to solve the issue of large-scale grid-interfaced EV charging [17]. It is a demand side management technique that encourages the car owners to plug-in their EVs more frequently during the off-peak time period by offering a lower tariff. This solution has the potential to reduce peak demand, particularly in the evenings, resulting in decreasing thermal and voltage issues in LV networks.

A solar hybrid system made up of PV and BES can be used to improve voltage levels in LV networks with PV and EV connections. The small solar hybrid system (kW range) is widely integrated with the main grid via a single-phase grid-tied hybrid inverter. This inverter is similar to a PV inverter, but it also includes the battery controller in a single unit. However, it was discovered that small-scale grid-tied hybrid inverters on the present market do not include the automatic Volt-Var control function during on-grid operation, such as the product of solar hybrid inverter as found in [18].

Contribution: This paper offers a voltage controller for a grid-tied hybrid inverter to avoid both over-and under-voltage concerns in weak LV radial networks with significant PV and EV penetration. The voltage level at the PCC can be adjusted by exchanging P and Q between the grid-tied hybrid inverter and the main grid. To mitigate over-voltage problems during the high PV generation, it can be done in two states which are 1) Absorbing Q and 2) P curtailment by charging the battery. On the other hand, rather of injecting Q, the battery can feed the P into the network to prevent the under-voltage during the high demand from EV charging. Moreover, the amount of P and Q from grid-tied hybrid PV-battery system should be correctly adjusted to ensure that the voltage level is always within the statutory limits, while the power factor of grid-tied hybrid inverter is still in the acceptable range.

The goal of this research is to show how the proposed voltage control strategy performs through computer simulations in the DIgSILENT *PowerFactory*. In addition, the case studies are explored in two scenarios which are 1) short-term voltage changes (90 seconds timeframe) to evaluate the dynamic performance of the proposed voltage controller, and 2) long-term voltage changes (24-hour timeframe) to investigate the voltage control performance throughout the day.

2. VOLTAGE VARIATIONS IN LV RADIAL NETWORKS

The LV radial network with PV and EV connections is depicted in Fig. 1. Without a PV system, power flows only in one direction from the distribution transformer to the residential load. The power supplied by PV systems, on the other hand, has an effect on reverse power flow and voltage level. Furthermore, the heavy load consumption while charging an EV raises concerns about voltage drop. The voltage level change that occurs when a PV system and an EV are connected to a specific location of an LV radial feeder can be explained as follows.

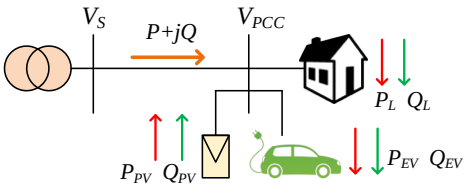

Fig. 1. Typical LV radial network with PV and EV.

Applied from [19], the voltage drop (ΔV) along the feeder is written as:

$$\Delta V = V_S - V_{PCC} = \frac{PR + QX}{V_{PCC}} \quad (1)$$

$$P = P_L + P_{EV} - P_{PV} \quad (2)$$

$$Q = Q_L + Q_{EV} - Q_{PV} \quad (3)$$

where, V_S is the voltage at the secondary side of transformer. V_{PCC} is the voltage at the PCC. P_L and Q_L represent the active power and reactive power consumed by the household electricity load, respectively. The active and reactive powers consumed by EV charging are denoted by P_{EV} and Q_{EV}, respectively. P_{PV} and Q_{PV} are active and reactive powers supplied by PV system, respectively. R and X are the resistance and the inductive reactance of the line feeder, correspondingly.

Assuming the voltage at the PCC is 1.0 p.u., so (1) can be approximated in per unit as:

$$\Delta V = \left(P_L + P_{EV} - P_{PV}\right)R + \left(Q_L + Q_{EV} - Q_{PV}\right)X \quad (4)$$

Over-voltage Issue in LV Netwroks with PV

According to the study of EV charging behavior in [7], most people charge their EVs at around 8 a.m. (before going to work) or at around 6 p.m. (after coming back home). As a consequence, the influence of EV charging on voltage changes could be ignored during peak PV generation at approximately midday. Then (4) can be written as:

$$\Delta V = \left(P_L - P_{PV}\right)R + \left(Q_L - Q_{PV}\right)X \quad (5)$$

The supplied power from PV system can reduce the terms (P-P_{PV}) and (Q-Q_{PV}) resulting in a drop in the value of ΔV. The voltage at PCC, V_{PCC}, will then be increase. Since PV systems typically operate at a power factor of 1.0 and have a Q_{PV} of zero, the voltage change is mainly driven by P injection from the PV system. If the P_{PV} exceeds the P_L, the reverse power flow occurs causing the voltage level to increase along the feeder.

Under-voltage Issue in LV Networks with EV

It was found that the most frequent first charge time of residential EVs started in the early morning or in the late afternoon [7]. As a result, the effect of PV power on voltage changes may be excluded. Furthermore, as residential houses in many countries have the high demand in the evening. The additional power consumption by EV charging can top up the peak demand, resulting in a significant voltage drop particularly at the end of feeder.

In a case of EV charging in the evening, (4) is thus expressed as:

$$\Delta V = \left(P_L + P_{EV}\right)R + \left(Q_L + Q_{EV}\right)X \quad (6)$$

The active and reactive power consumptions of EV charging can raise the terms (P+P_{EV}) and (Q+Q_{EV}) increasing the value of ΔV while decreasing the value of V_{PCC}. Due to EV chargers normally operate at unity power factor (Q_{EV} is zero), the drop in voltage level is caused mainly by the usage of P_{EV} when the EV is charging. If the amount of P_{EV} is particularly high, it has the potential to increase the voltage drop along the LV feeder, making the V_{PCC} to fall below the allowance value.

The voltage level in LV networks can be improved by upgrading the feeder line with lower R and X. However, this approach is expensive and must be implemented by DNOs. Another way to mitigate over-voltage is to reduce reverse power in the network which can be done by: 1) Curtailing the P_{PV}, 2) Absorbing Q_{PV} from the network into the PV system and 3) Increasing the load demand which can be achieved by charging either EV or BES system. Similarly, the under-voltage can be prevented by 1) Injecting Q_{PV} into the network if PV power is available, and 2) Lowering the load demand by enabling the BES to discharge power for load compensation.

Estimate Voltage Changes by Voltage Sensitiviy Ratios

The voltage sensitivity to a change in either P or Q at a PCC bus is used to determine the PCC voltage deviation. Individual bus sensitivity is calculated using network impedances, which vary according to line parameters and network topology. [20]. The inverse of the Jacobian matrix, J, is used to calculate the sensitivity ratios across the network. It was found that the voltage magnitude, V, and voltage angle, δ, are state variables that vary in response the changes of P and Q at a specific bus.

From the Newton-Raphson power flow calculation, it was found that:

$$\begin{bmatrix}\Delta P \\ \Delta Q\end{bmatrix} = \begin{bmatrix}J\end{bmatrix}\begin{bmatrix}\Delta\delta \\ \Delta V\end{bmatrix} = \begin{bmatrix}\partial P/\partial\delta & \partial P/\partial V \\ \partial Q/\partial\delta & \partial Q/\partial V\end{bmatrix}\begin{bmatrix}\Delta\delta \\ \Delta V\end{bmatrix} \quad (7)$$

The sensitivity matrix is then calculated from:

$$\begin{bmatrix}\Delta\delta \\ \Delta V\end{bmatrix} = \begin{bmatrix}J\end{bmatrix}^{-1}\begin{bmatrix}\Delta P \\ \Delta Q\end{bmatrix} = \begin{bmatrix}\partial\delta/\partial P & \partial\delta/\partial Q \\ \partial V/\partial P & \partial V/\partial Q\end{bmatrix}\begin{bmatrix}\Delta P \\ \Delta Q\end{bmatrix} \quad (8)$$

Based on Fig. 1, the deviation of voltage level at the PCC, ΔV_{PCC}, from the changes of P and Q at the PCC, which are ΔP and ΔQ, respectively, can be calculated by applying voltage sensitivity ratios ($\partial V/\partial P$ and $\partial V/\partial Q$) as:

$$\Delta V_{PCC} = \left[\partial V/\partial P\right]\times\Delta P + \left[\partial V/\partial Q\right]\times\Delta Q \quad (9)$$

If the ΔV_{PCC} is known, the $\partial V/\partial P$ and $\partial V/\partial Q$ are used to calculate the amount of P and Q required to support the voltage control. In addition, the ΔP can be obtained by curtailing PV power, charging EV and charging or discharging BES. The ΔQ, on the other hand, can be

achieved by exchanging the Q between the grid-tied hybrid inverter and the main grid.

Note that the positive sign means the power is supplied to the main grid, whilst the negative sign means the power is absorbed from the main grid.

3. GRID-TIED HYBRID INVERTER

Fig. 2 (a) presents a single-phase grid-tied hybrid inverter which is wildly used for small-scale hybrid PV – battery systems which capacities less than 5 kW. The grid-tied hybrid inverter, as shown in Fig. 2 (b), is typically based on voltage source converter that includes two DC/DC converters and a grid-tied DC/AC inverter. A PV panel - side DC/DC converter uses the maximum power point tracking (MPPT) algorithm to capture the maximum solar power, whereas a battery - side DC/DC converter can provide bi-directional power flow to support charging/discharging energy storage control.

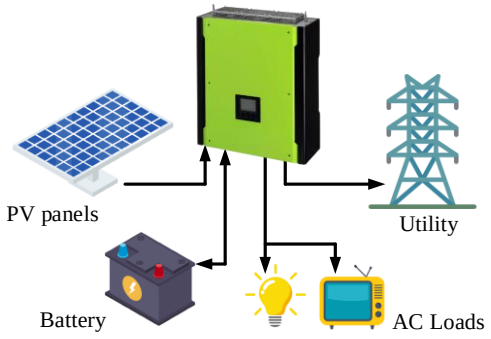

(a) Typical hybrid PV-battery structure

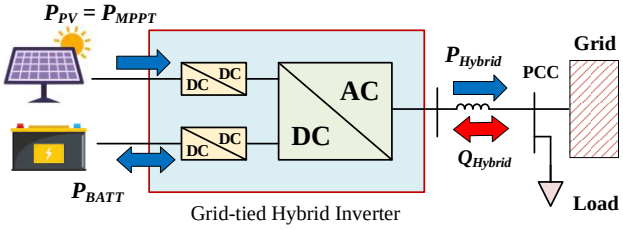

(b) Block diagram of grid-tired hybrid inverter

Fig. 2. Grid-tied hybrid PV-battery system.

This grid-tied hybrid inverter can work both on-and off-the grid. When connected to the grid, it acts as a grid following inverter, but when the main grid fails, it acts as a grid forming inverter to maintain stable voltage and frequency. The grid-side DC/AC inverter converts DC power from PV or battery to AC power and uses grid interface control to synchronize with the LV system. Apart from injecting power into the grid, the grid-side DC/AC inverter may draw power from the main grid and use it to charge the battery when the PV system is not available.

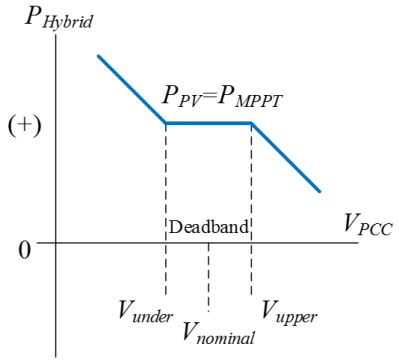

(a) $P(V)$ of hybrid inverter

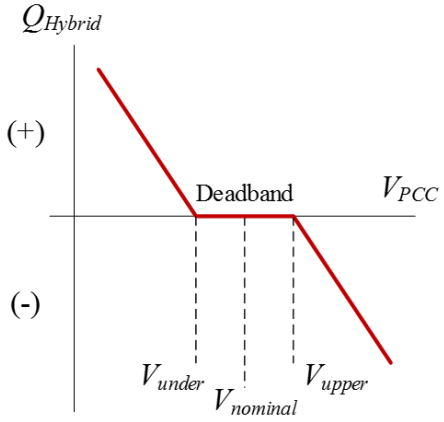

(b) $Q(V)$ of hybrid inverter

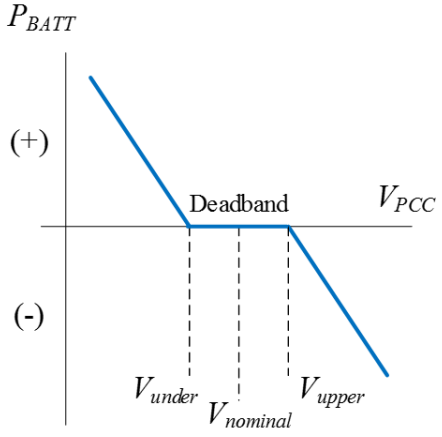

(c) $P(V)$ of battery

Fig. 3. $P(V)$ and $Q(V)$ controls of grid-tied hybrid inverter and battery.

It was found that most residential hybrid PV-battery systems use the single-phase grid-tied inverters, which generally operate in MPPT mode with the unity power factor and are unable to offer P and Q supports to deal with the voltage variations in the LV distribution networks. When the voltage at PCC is either higher or lower than

permissible values, the grid-tied hybrid inverter is typically disconnected from the main grid by its voltage protective device, resulting in a loss of energy supplied by PV or battery.

The battery-side DC/DC converter does not charge or discharge the battery when the level of state of charge (SoC) is between the minimum limit (SoC_{min}) and the maximum limit (SoC_{max}). Furthermore, the small-scale hybrid inverter will automatically charge the battery only when SoC is lower than SoC_{min}, or at a specified time if the duration is pre-set.

4. VOLTAGE CONTROL STRATEGY

P(V) and Q(V) droop controls

Droop control techniques are applied in this work to adjust active power and reactive power from grid-tied hybrid inverter, which are P_{Hybrid} and Q_{Hybrid}, respectively, for voltage control at the PCC. It begins to provide voltage control when the PCC voltage exceeds the upper limit (V_{upper}) or falls below the lower limit (V_{under}). Fig. 3 (a) and (b) show the relationship between the grid-tied hybrid inverter's outputs, P_{Hybrid} and Q_{Hybrid}, and the PCC voltage level, V_{PCC}.

Due to grid-tied hybrid inverters normally feed PV power at the maximum power point ($P_{PV} = P_{MPPT}$), the change of active power output is performed by adjusting the battery power, P_{BATT}, as can be written as:

$$P_{Hybrid} = P_{PV} + P_{BATT} \tag{10}$$

The $P(V)$ control capability depends on the battery's charging/discharging capacity, while the change of Q_{Hybrid} for providing voltage control is restricted by the hybrid inverter's power factor limit, PF_{Hybrid}. The maximum allowable reactive power, $Q_{Hybrid}^{\max}$, is calculated based on:

$$Q_{Hybrid}^{\max} = P_{Hybrid} \tan^{-1}\left(PF_{Hybrid}\right) \tag{11}$$

In the absence of the sun (P_{PV} is 0), the grid-tied hybrid inverter only controls the P_{BATT}, to inject or absorb P, for the voltage control without employing Q compensation (Q_{Hybrid} is 0).

To mitigate the over-voltage, the grid-tied hybrid inverter has to reduce P_{Hybrid} and absorb the Q_{Hybrid} from the main grid. As of (10), the P_{Hybrid} can be decreased by allowing the battery to charge the electricity (P_{BATT} is negative value). The quantity of P_{BATT} and Q_{Hybrid} is then estimated using the droop control approaches, as follows:

If $V_{PCC} > V_{upper}$, then

$$P_{BATT} = -\frac{\left(V_{PCC} - V_{upper}\right)}{K_P} \tag{12}$$

$$Q_{Hybrid} = -\frac{\left(V_{PCC} - V_{upper}\right)}{K_Q} \tag{13}$$

where, K_P and K_Q are the droop gains that can be applied with $\partial V/\partial P$ and $\partial V/\partial Q$, respectively.

On the other hand, the grid-tied hybrid inverter can avoid the under-voltage by raising P_{Hybrid} and injecting Q_{Hybrid} into the main grid. The battery's discharging power (P_{BATT} is positive value) can raise the value of P_{Hybrid}. Hence, the amount of P_{BATT} and Q_{Hybrid} for under-voltage control is determined as follows:

If $V_{PCC} < V_{under}$, then

$$P_{BATT} = -\frac{\left(V_{PCC} - V_{under}\right)}{K_P} \tag{14}$$

$$Q_{Hybrid} = -\frac{\left(V_{PCC} - V_{under}\right)}{K_Q} \tag{15}$$

From (12) and (14), the change in P_{BATT} as a function of V_{PCC} is presented in Fig 3 (c).

Two-state voltage control algorithm

The grid-tied hybrid PV-battery system begins to provide voltage control when either $V_{PCC} > V_{upper}$ or $V_{PCC} < V_{under}$. Moreover, the Q support is only operated when the PV power is available. The voltage control strategy for preventing voltage problems can be divided into two states, as follows;

State 01: The grid-tied hybrid inverter only supports reactive power control, Q_{Hybrid}, while the PV power is at the MPPT mode. The value of Q_{Hybrid} is calculated by using (13) and (15). In this state, the battery is in the standby mode, with no charge/discharge action, and $SoC_{\min} < SoC < SoC_{\max}$. The over- and under-voltage control in state 01 is presented in Fig. 4 (a) and (b), respectively.

State 02: The grid-tied hybrid inverter provides the reactive power support until the value of $|Q_{Hybrid}|$ reaches the power factor limit, $Q_{Hybrid}^{\max}$. In this state, the PV is still in the MPPT mode. If V_{PCC} exceeds V_{upper}, the value of P_{Hybrid} is curtailed by letting PV power to charge the battery through the battery-side DC/DC converter. The battery can support the over-voltage control until $SoC \geq SoC_{\max}$. In contrast, if $V_{PCC} < V_{under}$, the battery raises the value of P_{Hybrid} by discharging power into the main grid. The battery can associate the under-voltage control until $SoC \leq SoC_{\min}$. The over-and under-voltage controls in state 02 are shown in Fig. 4 (c) and (d), respectively. Moreover, the flow charts of proposed two-state voltage control are demonstrated in Fig. 5.

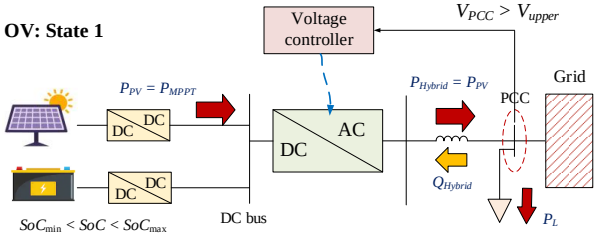

(a) Over-voltage control: State 01.

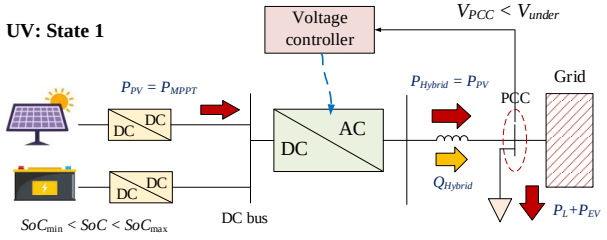

(b) Under-voltage control: State 01

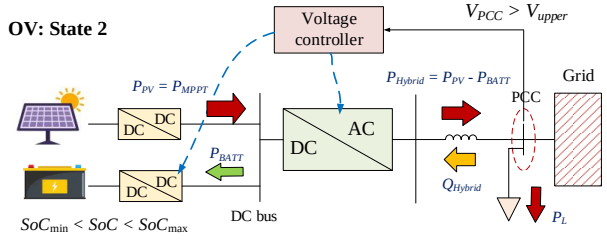

(c) Over-voltage control: State 02.

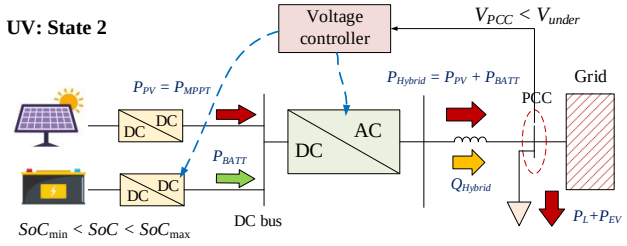

(d) Under-voltage control: State 02.

Fig. 4. Two-state voltage control of grid-tied hybrid inverter.

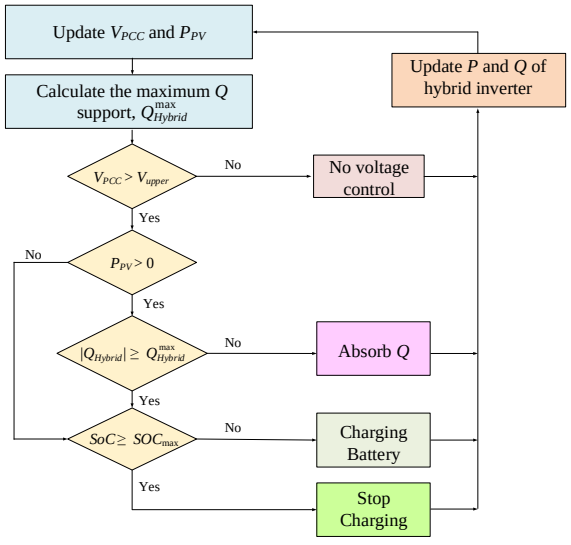

(a) Over-voltage control.

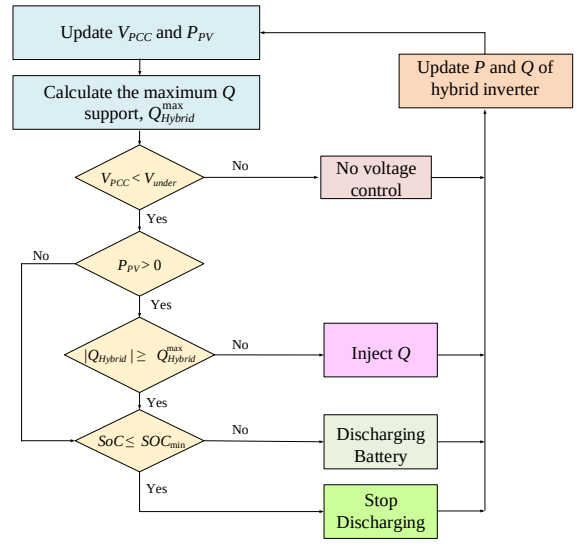

(b) Under-voltage control

Fig. 5. Flow charts of over-and under-voltage control approaches.

Modelling of grid-tied hybrid inverter with voltage controller

The dynamic responses of purposed voltage control strategy are observed by using *RMS* transient simulations in DIgSILENT *PowerFactory* environment. The grid-tied hybrid PV-battery system is represented as a static generator [21] that performs like a constant current source, as illustrated in Fig. 6. The control system is based on *dq* rotating reference frame and uses a phase lock loop (PLL) for grid synchronization. The real and imaginary components of grid-tied hybrid inverter's current output, i_{Hybrid}, are determined as follows:

$$\begin{aligned} \mathrm{Re}\left[i_{Hybrid}(t)\right] &= i_{d,ref}(t)\cdot\cos\theta(t) - i_{q,ref}(t)\cdot\sin\theta(t) \\ \mathrm{Im}\left[i_{Hybrid}(t)\right] &= i_{d,ref}(t)\cdot\sin\theta(t) + i_{q,ref}(t)\cdot\cos\theta(t) \end{aligned} \quad (16)$$

where, $i_{d,ref}$ and $i_{q,ref}$ are sent from active power (P) controller and reactive power (Q) controller, respectively. θ is the voltage angle of PCC bus measured by the PLL [22].

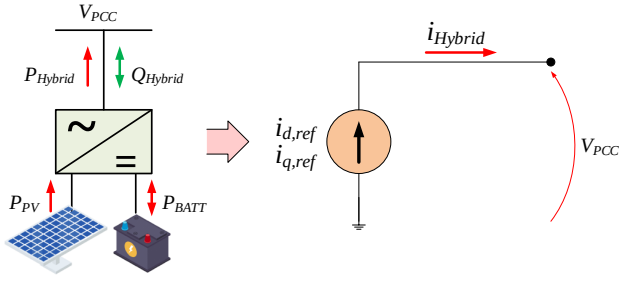

Fig. 6. Model of grid-tied hybrid PV-battery system.

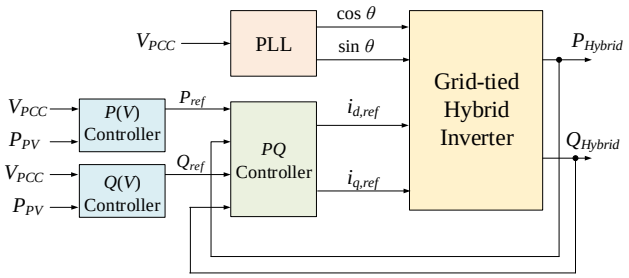

Fig. 7. Voltage controller structure.

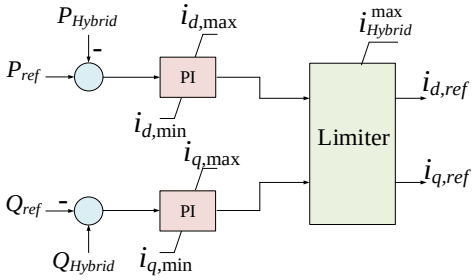

Fig. 8. *PQ* controller.

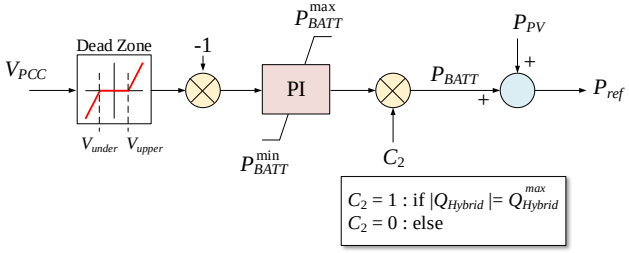

(a) *P*(*V*) controller

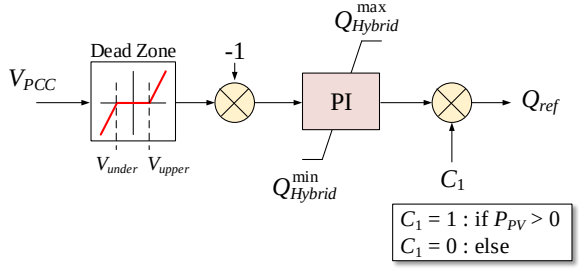

(b) *Q*(*V*) controller

Fig. 9. Voltage control loop.

The voltage controller structure of grid-tied hybrid inverter is presented in Fig. 7. The outer control loop consists of *P*(*V*) and *Q*(*V*) controllers used for voltage control, while the inner control loop is the *PQ* controller used for *P* and *Q* controls. As illustrated in Fig. 8, the *PQ* controller consists of *P* controller and *Q* controller. It is a close-loop controller that adjusts the P_{Hybrid} and Q_{Hybrid} of grid-tied hybrid inverter via the control of $i_{d,ref}$ and $i_{q,ref}$. The error signals in the *PQ* controller are compensated by using PI controllers. Moreover, the limiter is introduce to ensure that the grid-tied hybrid inverter delivers the apparent power within its capacity.

Fig.9 depicts the voltage control loop to regulate the values of P_{ref} and Q_{ref} of *PQ* controller. Under normal condition, there is no power supporting by the battery. The *P* reference (P_{ref}) is defined by the PV power delivered from the MPPT operation. To maintain a unity power factor, the *Q* reference (Q_{ref}) is set to zero.

When V_{PCC} exceeds or falls below the threshold values, the battery will provide active power compensation to support the voltage control. Therefore, the P_{ref} is the sum of P_{PV} and P_{BATT}. The P_{BATT} is controlled by a PI controller and has a charge/discharge power limit. Similarly, the Q_{ref} is controlled by a PI controller and is limited by the power factor constraint as determined by (11). It can be observed that if PV is not available (P_{PV} = 0), the Q_{ref} returns to zero and the voltage support is provided only by the battery power adjustment in the *P*(*V*) controller.

The control performances of the grid-tied hybrid inverter with the proposed two-state voltage control algorithm, based on *P*(*V*) and *Q*(*V*) droop controls, will be investigated using computer simulations in DIgSILENT *PowerFactory* environment. A weak LV distribution network with significant PV generating and EV charging capacities serves as the test system. Over- and under-voltage situations are created by raising the PV output of the grid-tied hybrid PV-battery system during the day and increasing EV charging during the night, respectively. When the PCC voltage level is greater or lower than the threshold values, the voltage is controlled by the grid-tied hybrid inverter with the proposed voltage controller. The values of supporting *P* and *Q* can be estimated using voltage sensitivities at the PCC bus. In addition, the case studies are investigated in two timeframes: 1) short-term voltage changes to analyze the proposed voltage controller's dynamic performance in milliseconds, and 2) long-term voltage changes to investigate the voltage control performance over a 24-hour period.

5. TEST SYSTEM

The test system is a residential house, which consists of a 5kW/5kWh hybrid PV-battery system and an EV, connected at the end of a 220 V, 50 Hz single-phase radial feeder, as illustrated in Fig. 10. The system is relatively weak due to the line impedance is quite high. Assume the residential EV is a small battery-powered type with the maximum demand of around 3 kW for slow charging while the peak PV production is approximately 3 kW. Moreover, the voltage sensitivity ratios at the PCC bus are $\partial V/\partial P$ = 0.04 p.u./kW and $\partial V/\partial Q$ = 0.037 p.u./kVar, correspondingly.

As the Thailand Grid Code defines a permit voltage range of 0.9 p.u. to 1.1 p.u. [23], the grid-tied hybrid inverter will start the voltage control when the PCC voltage level is above V_{upper} of 1.09 p.u. and falls below V_{under} of 0.91 p.u.. Under normal condition, the grid-tied hybrid PV-battery operates at the unity power factor (Q_{Hybrid} = 0). On

the other hand, the grid-tied hybrid inverter can provide Volt-Var control by varying the power factor between 0.9 leading and 0.9 lagging. Additionally, the *Q* compensation is only enabled when the PV generation is available.

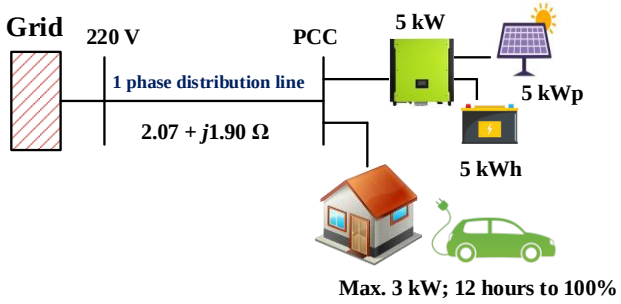

Fig. 10. Test system.

At initial condition, the battery is in the standby mode which the *SoC* is 30%. The percentages of $SoC_{\min}$ and $SoC_{\max}$ are 20% and 100%, respectively. After the *Q* of grid-tied hybrid inverter hits the power factor limit of 0.9 or PV production is absent, the battery will start supporting voltage control when the V_{PCC} is more than V_{upper} or less than V_{under}. The change of battery power is determined by the PCC voltage level while the changing/discharging power is restricted by the size of grid-tied hybrid inverter, which is 5 kW.

6. CASE STUDIES AND SIMULATION RESULTS

Increased PV generation and increased EV charging are used to address over-and under-voltage issues in the test system, respectively. In this study, the voltage control by adjusting *P* and *Q* from grid-tied hybrid PV-battery system is exercised in two different scenarios, depending on the duration of voltage changes, as followings:

Case 1) Short-term voltage variations

Case 2) Long-term voltage variations

Case 1 aims to demonstrate the dynamic performances of the proposed voltage controller in Section 4 when dealing with the fast voltage fluctuations, including both under-and over-voltage issues. The total simulation time is 90 seconds while the sampling time is 0.01 s. The voltage control responds can be investigated using *RMS*-transient simulations in DIgSILENT *PowerFactory* environment. The change of battery *SoC* is not mentioned in this scenario, due to the very short timeframe.

The objective of Case 2 is to explore how the two-state voltage control strategy proposed in Section 4 is used to handle over- and under-voltage changes throughout the day. The measuring interval is 1 minute and the monitoring period is 24 hours. In DIgSILENT *PowerFactory* environment, the voltage management in the weak LV network is tested for a full day using quasi-dynamic simulations, which are time-sweep load flow computations. In this scenario, the variations in battery *SoC* are also illustrated.

Case 1) Short-term voltage variations

The rapid changes of PV production of grid-tied hybrid PV-battery system and residential load consumption are applied in this scenario, as shown in Fig. 11 (a). Within 10 seconds, PV power climbs from zero to 3 kW, while load demand grows from 0.4 kW to 3.5 kW. The PV generation is available for 45 seconds, whereas the duration of load change is about 35 seconds. The load starts to increase as the PV output decreases. Without the voltage control, the results of *RMS*-transient simulations in Fig. 11 (b) reveal that when the PV generation is large, the PCC voltage level surpasses the acceptable upper limit (1.1 p.u.) between t = 9 seconds and t = 42 seconds. In contrast, when the load demand is too high due to the additional EV charging, the PCC voltage level drops below the acceptable lower limit (0.9 p.u.) between t = 48.5 seconds and t = 72.5 seconds.

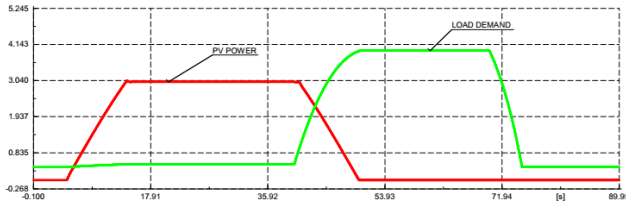

(a) Load and PV generation profiles (kW)

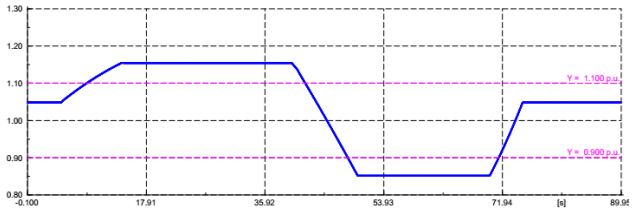

(b) The voltage level at the PCC (p.u.)

Fig. 11. Load profile, PV generation profile and voltage level at the PCC, without voltage control in Case 1.

After applying voltage controller into the grid-tied hybrid inverter, the simulation results in Fig. 12, show that the proposed voltage control strategy can effectively deal with short-term voltage variations at the PCC, avoiding either under- or over-voltage issues caused by increased PV generation and load consumption, as shown in Fig. 12 (a). The grid-tied hybrid inverter suddenly absorbs the *Q* until it reaches the power factor limit of 0.9, at which point the Q_{Hybrid} is roughly 1.2 kVar, as found in Fig. 12 (b) and (c), respectively. After that, if the voltage level remains above the upper limit, the *P* output of grid-tied hybrid inverter is then curtailed by charging the battery. It was found that the battery charging power is around 0.68 kW to reduce the P_{hybrid} and to avoid the over-voltage situation (see Fig. 12 (b)).

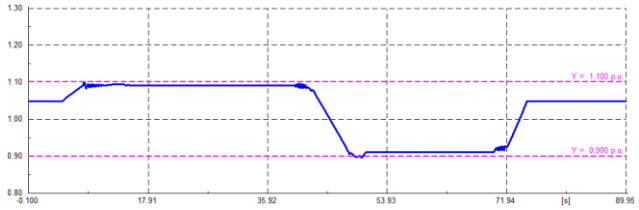

(a) The voltage level at the PCC (p.u.)

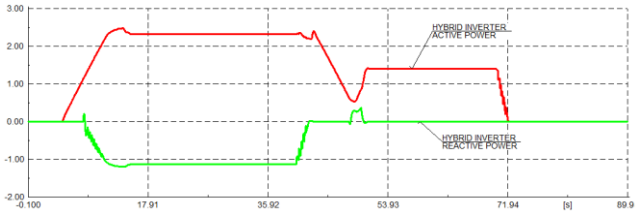

(b) *P* and *Q* from grid-tied hybrid inverter (kW, kVar).

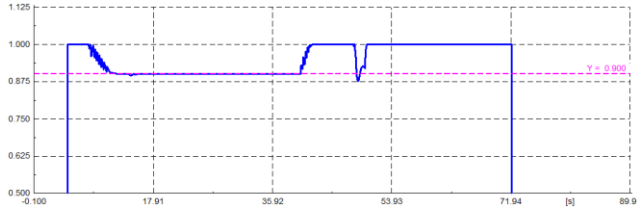

(c) Power factor of grid-tie hybrid inverter

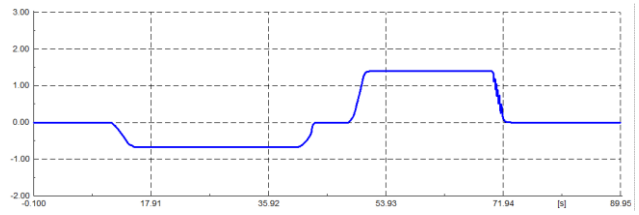

(d) Battery power

Fig. 12. The changes of PCC voltage level, outputs of grid-tied hybrid inverter and battery power, with voltage control in Case 1.

From Fig. 12 (b) and (c), it was observed that PV power is still available as the beginning of heavy load scenario, at time between 40 and 50 seconds. Hence, the grid-tied hybrid inverter will inject the extra *Q* into the main grid to prevent the under-voltage issue. The Q_{Hybrid} is only fed 0.266 kVar for nearly 2 seconds, due to the PV output being rather low (about 0.53 kW). After the sun has gone down or the grid-tied hybrid inverter has supplied *Q* to the point where it exceeds the $Q_{Hybrid}^{\max}$, the battery power of approximately 1.401 kW is then discharged to compensate for the electricity required by EV charging, as demonstrated in Fig. 12 (d). As a consequence, the PCC voltage level remains within the statutory ranges.

Case 2) Long-term voltage variations

The daily PV power profile and load profile, as illustrated in Fig. 13 (a), are employed in this case. In addition, assume the EV has a *SoC* level of 40 % remaining and has been plugged in for slow charging for nearly 8 hours since 18:00. The results from quasi-dynamic simulations in Fig. 13 (b) show that, without voltage control, the over-voltage issue occurs between 8:35 and 16:00, due to the excessive power from the highly PV production. The under-voltage problem, on the other hand, happens between 18:00 and 22:35, due to heavy load consumption during the period of constant current charge of EV.

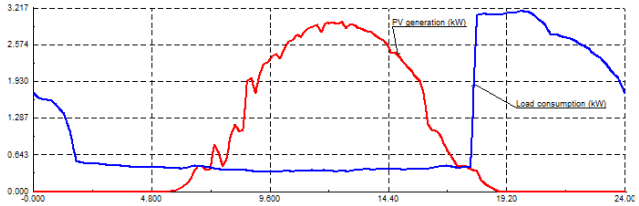

(a) Load and PV generation profiles (kW)

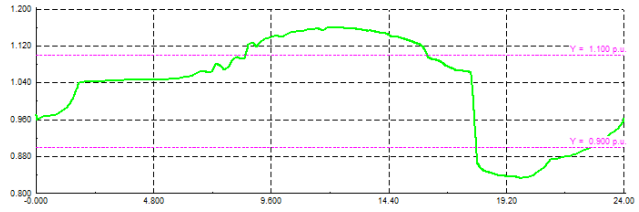

(b) The voltage level at the PCC (p.u.)

Fig. 13. Load profile, PV generation profile and voltage level at the PCC, without voltage control in Case 2.

Fig. 14 shows the simulation results when the two-state voltage control strategy is applied to the grid-tied hybrid PV-battery system. It can be seen that the proposed voltage control method can successfully deal with the over- and under-voltage issues, which the PCC voltage level can stay within the Grid Code requirement (0.9 - 1.1 p.u.) for the entire day, as shown in Fig. 14 (a).

The changes in *P* and *Q* of grid-tied hybrid are illustrated in Fig. 14 (b) and (c), respectively. It was found that the grid-tied hybrid inverter with voltage controller begins to support the *Q* absorption at 8:00 in order to avoid the over-voltage. After 8:42, the individual *Q* control is no longer adequate and then the *P* curtailment from battery charging is requested, as found in Fig. 14 (e). The values of battery charging power and the *Q* supported by grid-tied hybrid inverter are estimated by using (11) to (14), which can maintain the power factor of grid-tied hybrid inverter from falling below 0.9 (see Fig. 14 (d)). The combination of *P* curtailment and *Q* absorption by grid-tied hybrid inverter successfully prevents the over-voltage problem until 15:28, when the level of battery's *SoC* reaches 96 %, as presented in Fig. 14 (f). Because the degree of over-voltage after 15:30 is relatively low, only *Q* compensation is sufficient to support voltage control. Since 16:00, the grid-tied hybrid PV-battery system has stopped voltage control and the grid-tied hybrid inverter resumes working at unity power factor with no *P* reduction.

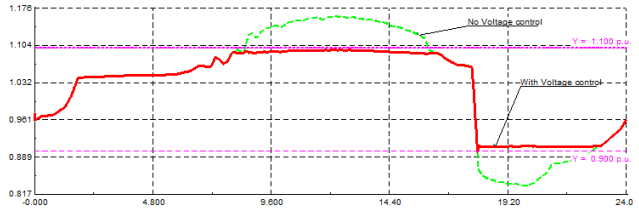

(a) The voltage level at the PCC (p.u.)

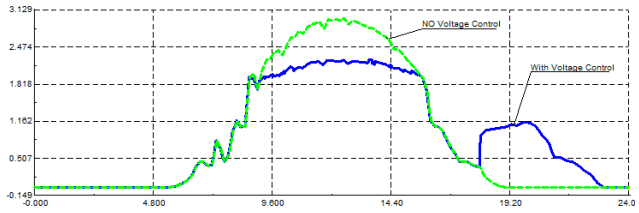

(b) *P* from grid-tied hybrid inverter (kW)

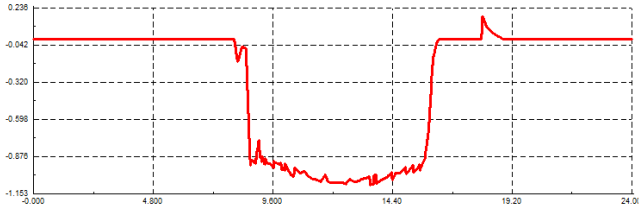

(c) *Q* from grid-tied hybrid inverter (kW)

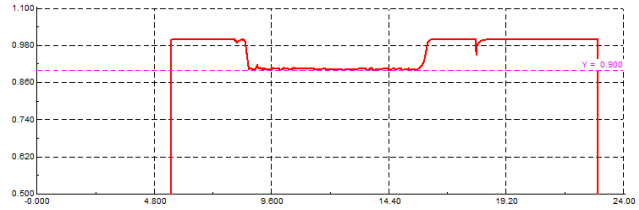

(d) Power factor of grid-tie hybrid inverter

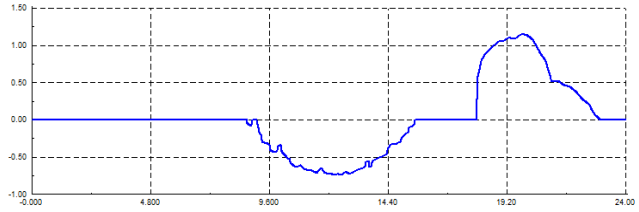

(e) Battery power (kW)

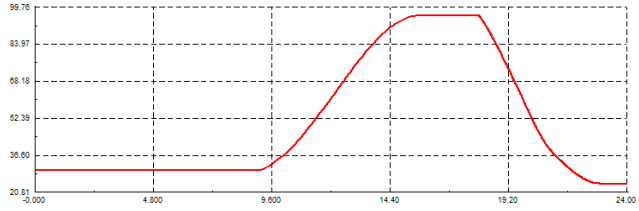

(f) % Battery *SoC*

Fig. 14. The changes of PCC voltage level, outputs of grid-tied hybrid inverter, battery power and % *SoC*, with voltage control in Case 2.

Since the EV starts charging power at 18:00 (see Fig. 13 (a)), the grid-tied hybrid PV-battery system will inject *P* and *Q* to avoid the PCC voltage level from falling below 0.9 p.u., as illustrated in Fig 14 (b) and (c). Between 18:00 and 19:00, the *P* output of grid-tied hybrid inverter is from the total amount of PV power and battery power while the value of *Q* injection is rather small due to the low PV production. After that, the sun has set, so the voltage is controlled solely by the battery's discharging power of roughly 1.1 kW, as shown in Fig. 14 (e). The *P* support provided by battery can prevent the under-voltage successfully until the PCC voltage level is above the threshold value (> 0.91 p.u.), which occurs at 23:00. Then, the voltage control is disable with no *P* and *Q* supplied by grid-tied hybrid PV-battery system. From Fig. 14 (f), it was found that for nearly 5 hours of supporting under-voltage control, the level of battery's *SoC* significantly drops from 96 % to 24.4 %.

7. CONCLUSION

A voltage controller for a single-phase grid-tied hybrid inverter is introduced to avoid both over-and under-voltage concerns in weak LV networks with significant PV and EV penetrations. The two-state voltage control method of grid-tied hybrid inverter using *P*(*V*) and *Q*(*V*) droop controls is implemented for providing over-and under-voltage controls. The PCC voltage level can be controlled by exchanging *P* and *Q* between the grid-tied hybrid PV-battery system and the main grid. The *P* output can be adjusted via the battery's charge/discharge while the change of *Q* is restricted by the hybrid inverter's power factor limit. According to the simulation results, the grid-tied hybrid PV-battery system with voltage controller can effectively handle over- and under-voltage issues, both short-and long term voltage changes, which the PCC voltage level always stays within the statutory limits. Since there are no voltage issues, it can increase the hosting capacity of PV and EV connections in LV distribution networks.

ACKNOWLEDGMENT

This work is in "Automatic voltage control for grid-connected single phase hybrid inverter to preventing over-voltage problems in distribution networks with photovoltaic/Battery systems" project (grant number R2564E002) supported by Centre of Excellence on Energy Technology and Environment (CeTe) and Faculty of Engineering, Naresuan University, Thailand.

REFERENCES

[1] Ismail, A. M.; Ramirez-Iniguez, R.; Asif, M.; Munir, A.B. and Muhammad-Sukki, F. 2015. Progress of solar photovoltaic in ASEAN countries: A review. In *Renewable and Sustainable Energy Reviews*. August. Elsevier Publisher.

[2] Industry Report in Automotive (2020). ASEAN Electric Vehicle Market-growth, Trends, Covid-19 Impact, and Forecasts (2021-2026). Mordor Intelligence.

[3] Tonkoski, R.; Turcotte, D. and EL-Fouly, T. H. M. 2012. Impact of High PV Penetration on Voltage Profiles in Residential Neighborhoods. In *IEEE Transactions on Sustainable Energy*, vol. 3, no. 3, pp. 518-527.

[4] Quirós-Tortós, J.; Ochoa, L.F.; Alnaser, S.W. and Butler, T. 2016. Control of EV Charging Points for Thermal and Voltage Management of LV Networks. In *IEEE Transactions on Power Systems*, vol. 31, no. 4, pp. 3028-3039.

[5] Quirós-Tortós, J.; Ochoa, L.F.; Alnaser, S.W. and Butler, T. 2018. Statistical Representation of EV Charging: Real Data Analysis and Applications. In *2018 Power Systems Computation Conference (PSCC)*, pp. 1-7.

[6] Schey, S.; Scoffield, D. and Smart, J. 2012. A First Look at the Impact of Electric Vehicle Charging on the Electric Grid in the EV Project. In *EVS26 International Battery, Hybrid and Fuel Cell Electric Vehicle Symposium*. Los Angeles, California.

[7] Quiros-Tortos, J.; Ochoa, L.F. and Butler T. 2018. How Electric Vehicles and the Grid Work Together: Lessons Learned from One of the Largest Electric Vehicle Trials in the World. In *IEEE Power and Energy Magazine*, vol. 16, no. 6, pp. 64-76.

[8] Shayani, R. A. and de Oliveira, M. A. G. 2011. Photovoltaic Generation Penetration Limits in Radial Distribution Systems. In *IEEE Transactions on Power Systems*, vol. 26, no. 3, pp. 1625-1631.

[9] Wang, Y.; Zhang, P.; Li, W.; Xiao, W. and Abdollahi, A. 2012. Online Overvoltage Prevention Control of Photovoltaic Generators in Microgrids. In *IEEE Transactions on Smart Grid*, vol. 3, no. 4, pp. 2071-2078.

[10] Goqo, Z. and Davidson, I.E. 2018. A Review of Grid Tied PV Generation on LV Distribution Networks. In *2018 IEEE PES/IAS PowerAfrica*, pp. 907-912.

[11] Procopiou, A.T.; Petrou, K.; Ochoa, L.F.; Langstaff, T. and Theunissen, J. 2019. Adaptive Decentralized Control of Residential Storage in PV-Rich MV–LV Networks. In *IEEE Transactions on Power Systems*, vol. 34, no. 3, pp. 2378-2389.

[12] Hashemi, S.; Østergaard, J. and G. Yang, G. 2013. Effect of reactive power management of PV inverters on need for energy storage. In *IEEE 39th Photovoltaic Specialists Conference (PVSC)*, Tampa, FL, pp. 2304-2308.

[13] Bletterie, B.; Kadam, S.; Bolgaryn, R. and Zegers, A. 2017. Voltage Control with PV Inverters in Low Voltage Networks—In Depth Analysis of Different Concepts and Parameterization Criteria. In *IEEE Transactions on Power Systems*, vol. 32, no. 1, pp. 177-185, Jan.

[14] Deshmukh, S.; Natarajan, B and Pahwa, A. 2012. Voltage/VAR Control in Distribution Networks via Reactive Power Injection through Distributed Generators. In *IEEE Transactions on Smart Grid*, vol. 3, no. 3, pp. 1226-1234.

[15] Pachanapan, P. and Kanprachar, S. 2017. Voltage Level Management of Low Voltage Radial Distribution Networks with High Penetration of Rooftop PV Systems. In *GMSARN International Journal*. Vol. 11, pp. 16-22.

[16] S. Hashemi, J. Østergaard and G. Yang. A Scenario-Based Approach for Energy Storage Capacity Determination in LV Grids with High PV Penetration. In *IEEE Transactions on Smart Grid*, vol. 5, no. 3, pp. 1514-1522, May 2014.

[17] Zhao, Y.; Huang, H.; Chen, X.; Zhang, B.; Zhang, Y.; Jin, Y.; Zhang, Q.; Cheng, L. and Chen, Y. 2019. Charging Load Allocation Strategy of EV charging station consider charging mode. In *World Electric Vehicle Journal*, vol. 10, issue 2.

[18] User's Manual (2021). PH1800 Plus Series High Frequency On/Off Grid Hybrid Solar Inverter. Must Solar.

[19] Jenkins, N.; Ekanayake, J.B. and Strbac, G. 2010. *Distributed Generation*, 1st ed. The Institution of Engineering and Technology, chapter 3.

[20] Le, A.D.T.; Muttaqi, K.M.; Negnevitsky, M. and Ledwich, G. Response coordination of distributed generation and tap changers for voltage support. In *Australasian Universities Power Engineering Conference*, pp. 1-7.

[21] PowerFactory User's Manual (2018). Technical Reference Documentation: Static Generator. DIgSILENT GmbH.

[22] PowerFactory User's Manual (2018). Technical Reference Documentation: Phase Measurement Device. DIgSILENT GmbH.

[23] Provincial Electricity Authority (PEA). 2016. Interconnection Code. Thailand.